

Electromicrogravimetric Study of the Effect of Cl⁻ Anions on Thallium Underpotential Deposition Onto Gold

Antonio Montes-Rojas*^{1,2} and Eric Chainet¹

¹Laboratoire d'Electrochimie et de Physico-chimie des Matériaux et des Interfaces-UMR INPG-CNRS 5631 associée à l'UJF. École Nationale Supérieure d'Electrochimie et d'Electrometallurgie de Grenoble, Domaine Universitaire, 1130 rue de la Piscine, BP 75, 38402 St. Martin d'Hères Francia

²Centro de Investigación y Estudios de Posgrado. Facultad de Ciencias Químicas, Universidad Autónoma de San Luis Potosí, Av. Dr. Manuel Nava No. 6, Zona Universitaria C.P. 78210, San Luis Potosí, S.L.P. México, Teléfono: (0144) 8262440/46, extensión 561, Fax: (0144) 8262372, e-mail: antonio.montes@uaslp.mx

Recibido el 28 de enero del 2005; aceptado el 29 de noviembre del 2005

Abstract. The effect of chloride adsorption on underpotential deposition of thallium onto gold electrode was studied using cyclic voltammetry coupled with microgravimetry. The results obtained suggest the existence of two potential regions with different processes occurring during Tl UPD in the presence of anions. In the first zone, at low coverage, there are two simultaneously occurring processes: desorption of all chloride atoms, which are adsorbed on the gold substrate prior to the onset of Tl UPD, and thallium adsorption on the energetically most favorable sites (grain boundaries, steps, etc) present on the electrode surface. During these processes a strong interaction among thallium atoms is induced by the presence of chloride atoms on the adjacent sites. This strong interaction generates sharper current peaks in the voltammogram, associated with the above processes, and their displacement towards cathodic potentials proportional to the anion concentration. However, in the second potential zone at high coverage, the adsorption of thallium atoms takes place on the least accessible sites (terraces) on the gold substrate. In this type of sites, the effect of the presence of chloride atoms on the UPD process is unimportant.

Key words: electromicrogravimetry, underpotential deposition, thallium, adsorption, chloride.

Resumen. El efecto de la co-adsorción de los aniones cloruro sobre la formación del depósito en subpotencial de talio sobre electrodo de oro fue estudiado por el acoplamiento de la voltamperometría cíclica a la microbalanza de cuarzo. Los resultados obtenidos ponen en evidencia dos zonas de potencial en las que ocurren procesos diferentes durante la formación del depósito UPD de talio en presencia de cloruros. En la primera zona, a bajos recubrimientos, se produce simultáneamente la desorción de todos los iones cloruro, que ya recubrían la superficie del electrodo antes de iniciar la formación de la monocapa de talio, y la adsorción de los átomos metálicos de talio en los sitios energéticamente más accesibles (tipo escalón, hueco, etc.). Durante este proceso se produce una fuerte interacción entre los átomos metálicos adsorbidos sobre el sustrato debido a la presencia de los aniones cloruros adsorbidos que se mantienen en los sitios adyacentes. Esta interacción se refleja en picos de corriente más agudos y a un desplazamiento hacia potenciales menos positivos en el voltamperograma. Los resultados obtenidos muestran que este proceso es dependiente de la concentración del anión en solución. En cuanto a la segunda zona de potencial, a altos grados de recubrimiento, sólo se produce la adsorción de los átomos de talio en los sitios menos energéticamente accesibles (tipo terraza) sin una influencia importante de los iones cloruro.

Palabras clave: electromicrogravimetría, depósito a subpotencial, talio, adsorción, cloruro.

Introduction

The underpotential deposition (UPD) of a metal, defined as the deposition of a metal monolayer on a dissimilar metal substrate at a potential anodic of the Nernst potential for bulk deposition, has been a subject of intense theoretical and experimental interest [1, 2]. There are several reasons for this, for example:

- To obtain desired physicochemical properties in a metallic deposit, the formation process must be controlled with precision, and consequently, better knowledge of the initial stages (adsorption, nucleation and growth) of this metallic deposit should be acquired.
- Some UPD systems have been studied in a more detailed fashion because of the enhanced catalytic activity of certain chemical reactions of practical relevance [3].

Numerous bimetallic systems formed by a UPD process have been widely investigated since the underpotential deposition offers a unique possibility to form submonolayers of metal atoms at equilibrium conditions, and to vary their coverage by changing potential and concentration of the corresponding cations, i. e. a controlled modification of the surface properties.

The Tl /Au system is known to enhance the catalytic activity for oxygen reduction in acid media or for formaldehyde oxidation in alkaline solution [4, 5]. The thallium UPD on gold in the absence of anions has been the subject of numerous studies and their most relevant results are the following:

- Ionic metallic species transfer completely their charge to substrate.
- Monolayer formation begins with a decoration of steps and surface inhomogeneities (point defect, kinks sites, etc.).

iii) Terrace adsorption sites are occupied at relatively high coverage.

One of the aspects that have attracted an increasing interest is the role of anions in the UPD process. The effect of specific anion adsorption on UPD has since been discussed by a number of other research groups [6, 12]. However, no consistent interpretation has been proposed for these effects, although several mechanisms have been suggested.

Schmidt and Wuthrich [13] reported that halide ions formed a compound with the substrate that strongly inhibited the UPD of the metal monolayer. On the other hand, Kolb et al [14] and some other authors [15, 16] argued that halide interaction with the adsorbate was much stronger than with the substrate and thus influenced the UPD of the admetal. More recent studies using single crystal surfaces have demonstrated that concurrent anion adsorption at the electrode/solution interface, plays an important role in the ordering and growth of the UPD metal. In this case, some authors [17] accept that the mechanism for deposition can be outlined as follows. After the appearance of a preadsorbed state, the initial metal adsorption would give rise to a mixed MeAn (An = anion) adlayer which, in turn, during the second stage of deposition process would become a metallic monolayer covered by an anion adlayer. This mechanism has been proposed to explain experimental data about Cu UPD on Pt(111) in the presence of bisulfate, chloride or bromide. Obviously, an extension of these studies to other UPD systems is of interest.

The UPD process has been studied with a wide variety of techniques included the electrochemical quartz-crystal microbalance (EQCM).

In application of the EQCM, the change in surface mass Δm is calculated from the change in resonant frequency Δf using an equation derived by Sauerbrey [18, 19]:

$$\Delta m = -C_f \Delta f \quad (1)$$

where the constant $C_f = \frac{(\mu_q \rho_q)^{1/2}}{2f_o^2 \pi}$ depends only on the properties of the quartz resonator itself: μ_q and ρ_q are the shear modulus and density of quartz, respectively, and f_o is the fundamental resonator frequency.

This equation holds only under certain conditions such as that this assumption is reasonable if the resonant frequency shifts by no more than 2% from the fundamental. This condition is easily met in UPD systems, and all frequency changes reported here are well below this limit.

There is only one article on UPD of Tl on Au using EQCM, reported by Niece [20] who have found that, in contrast to the voltammograms, a potential-dependent frequency variation response does not follow the same mechanism for the adsorption and desorption, respectively, because of the remarkable hysteresis between the two processes. Additionally, in the potential region studied before the UPD formation, a process involving a loss of mass, associated with

the “desorption” of perchlorate anions, is clearly observed. This is a peculiar result since most of the works reported show that this anion adsorbs very weakly.

Notwithstanding these papers, there is no work on the mechanism of Tl UPD process on gold in the presence of anions.

Therefore, the results of thallium UPD on gold presented herein are obtained both in the presence and the absence of chloride. The UPD process is examined by EQCM coupled with cyclic voltammetry.

Experimental

1. Reagents

The supporting electrolyte used in this work was NaClO₄ 1 M solution, because of the known weak adsorption of perchlorate anion [21] on gold electrodes. Tl⁺ solutions were prepared by dissolving Tl₂(CO₃) salts in tridistilled water so that the metal ion concentration in the supporting electrolyte solution was 10⁻³ M. Anion effect was studied using reagent grade NaCl salt to make anion concentration range between 10⁻³ and 10⁻² M and avoid any formation of coordination complexes consisting of present metal ions. All solutions were adjusted to pH 3.5 using reagent grade HClO₄. In addition, prior to the realization of experiments, the solution was purged with high purity argon to remove dissolved oxygen and the same gas was used to maintain inert atmosphere during experiments.

2. Electrodes

Working electrodes (Maxtek) of 1.37 cm² geometric area were gold electrodes supported on polished quartz discs with titanium underlayer to improve gold adherence to quartz, vibrating in their own fundamental mode at 5 MHz. These electrodes were cycled using a voltammetric program at 100 mV/s rate in a supporting electrolyte solution in the absence of both metal ion and study anion [22-24]. The counter electrode was a platinum wire with a greater area than the working electrode. Saturated calomel (SCE) was used as reference electrode, and placed in a special recipient in contact with the working solution to avoid chloride anion addition to the solution.

3. Apparatus

Electrochemical experiments were carried out using a PAR potentiostat-galvanostat model 273A operated by M270 software. For *in situ* mass measurements, a Maxtek microbalance model 710 coupled to the potentiostat was used.

Finally, quartz microbalance was calibrated using thallium solution 10⁻³ M in acid media as has been announced by Fletcher [25]. Thus, the sensitivity constant C_f was 17.95 ± 0.25 ng Hz⁻¹ cm⁻² which approaches very closely the theoretical value of 18 ng Hz⁻¹ cm⁻² obtained through the expression 1. In addition, if the surface structure of the elec-

trodes is considered predominant (111), then the resulting densities of adsorption sites are of the order of 10^{15} sites/cm².

Results and Discussion

1. Characterization of the Electrodes

One of the first steps we made in this work was to apply a cyclic voltammetry treatment to sodium perchlorate in the absence of both thallium and chloride at high scan rate as suggested by some authors [22, 23]. This procedure gives rise to reproducible and well-defined voltammetric responses, which witnesses the quality of the electrodes and the cleanliness of working solutions.

Figure 1 shows a typical current-potential (*j*-*E*) curve obtained at an Au film electrode in 1 M Na₂SO₄ adjusted at pH 2 with H₂SO₄. The very small anodic current observed during the positive potential scan in region A (-500 to ca. +1000 mV) corresponds to the electrical double layer charging and the so-called "pre-oxide" region. The large wave in region B (ca. +1000 to +1500 mV) corresponds to anodic formation of the inert surface oxide. Scan reversal at +1500 mV just prior to O₂ evolution, results in rapid cessation of the anodic current followed by a cathodic peak in the region ca. +1200 to +700 mV, corresponding to reductive dissolution of oxide.

This curve was compared with those obtained by Hamelin for a typical Au(111) electrode [22, 23]. The typical current peaks are seen at +1053 and +1234 mV in the anodic potential scan, including $451 \pm 8 \mu\text{C cm}^{-2}$ for the oxide layer formation and at +865 mV in the cathodic potential scan with $446 \pm 9 \mu\text{C cm}^{-2}$ for the oxide layer reduction, which approaches very closely the theoretical value of $444 \mu\text{C cm}^{-2}$ of an Au(111) electrode.

In addition we obtained the X-ray diffraction spectrum of the gold layer deposited on quartz substrate in order to determine whether it was presenting a preferential orientation since

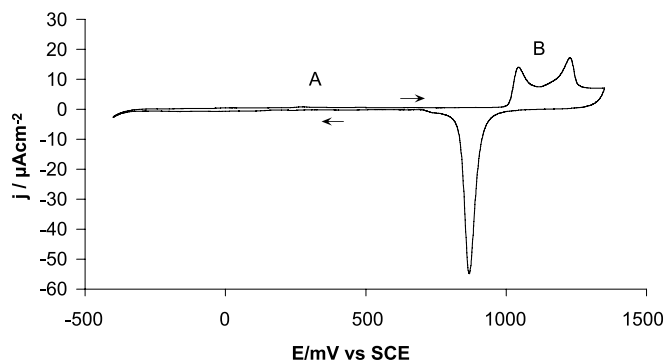


Fig. 1. Voltammetric curve of gold deposited on quartz (pseudo Au(111)) in 1 M Na₂SO₄ adjusted at pH 2 with H₂SO₄; scan rate, 5 mV s⁻¹. Zone A corresponds to the electrical double layer charge; zone B corresponds to anodic formation of the inert surface oxide.

the use of a well-defined electrode surface is important in this kind of study. These results showed that no titanium underlayer used to improve adherence between gold and quartz substrate is detected, just the presence of the quartz substrate and the gold layer with highly ordered Au(111).

Figure 2 shows the voltammetric and frequency-potential (Δf -*E*) curves recorded only for region A. During the positive scan from 600 mV to -400 mV, there is no detectable change in frequency or current corresponding to double-layer charge. However, a rapid decrease in the frequency (mass increase) and the current is observed at -400 mV of 2 Hz and $10 \mu\text{A cm}^{-2}$, respectively, corresponding probably to H_{ads} adsorption. Following scan reversal at -500 mV, the frequency remains constant, while the current increases rapidly; however, in the region ca. -350 to 0 mV a slow increase of frequency occurs concomitantly with the desorption of H_{ads}. Finally, the frequency returns to the original value in the double-layer region.

This result ensures that EQCM measurements in the present study correspond to Tl/Au UPD system in acid media.

2. Thallium UPD on Au in the Absence of Chloride

Figure 3 shows cyclic voltammetric curves obtained over the UPD and the OPD (Overpotential Deposition) region in the presence (a) and absence (b) of metallic ion in electrolyte solution.

On one hand, it is relevant to mention that the reduction of H⁺ at -685 mV (curve b) is strongly inhibited by adsorbed thallium similar to the bulk metal (curve a).

On the other hand, when there is a thallium ion in the solution, the electrode response changes. During the direct scan it is possible to note, for curve a, just one wave at -760 mV after the equilibrium potential *E*_N of the Tl⁺/Tl system (the equilibrium potential, *E*_N(Tl⁺/Tl), for this metallic ion concentration is -758 mV) corresponding to OPD process of thallium. In the reverse potential scan, only one peak is observed at -664 mV. According to its potential position, this peak can be related to the dilution process of massive deposit of thallium on the gold electrode.

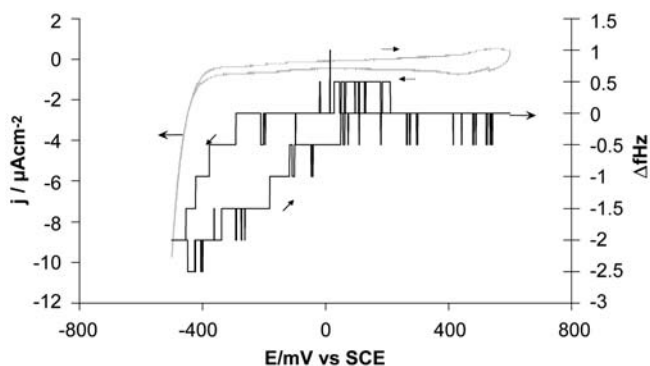


Fig. 2. (----) cyclic voltammogram and (—) concomitant change in frequency of the EQCM working electrode in NaClO₄ 1M at pH 3.5. The scan rate was 5 mV/s.

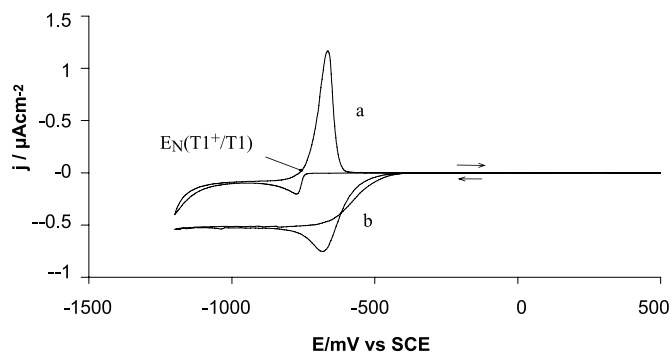


Fig. 3. Cyclic voltammograms obtained over the UPD and the OPD (Overpotential Deposition) regions in the presence (a) and absence (b) of metallic ion in electrolyte solution. The systems were: (a) Au/10⁻³ M Tl⁺ + 1 M NaClO₄ (pH 3.5) and (b) Au/NaClO₄ 1 M (pH 3.5). The potential scan was performed at 5 mV s⁻¹. The equilibrium potential, E_N(Tl⁺/Tl), for this metallic ion concentration is -758 mV.

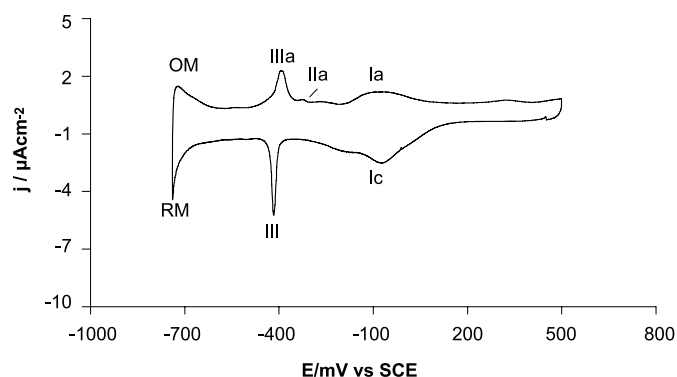


Fig. 4. Cyclic voltammogram of Tl UPD on gold substrate in 1 M NaClO₄ (pH 3.5) + 1 mM Tl⁺. Scan rate: 5 mV s⁻¹. The equilibrium potential, E_N(Tl⁺/Tl) for this metallic ion concentration is -758 mV.

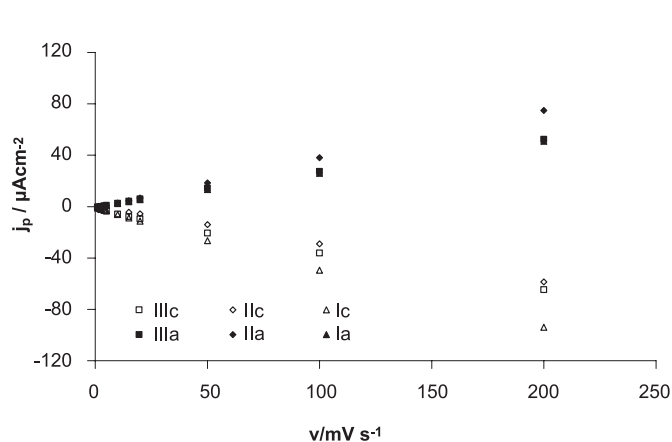


Fig. 5. j_p vs ν for peaks I, II and III of Au/10⁻³ M Tl⁺ system + 1 M NaClO₄ (pH 3.5). The electrode's area is 1.37 cm².

If the potential scan to UPD region is limited, the voltammetric response obtained is as shown in Figure 4.

During the direct scan in the UPD region three cathodic peaks can be observed at -89 (Ic), -373 mV (IIc, this peak is only observable in the voltammetric response at high scan rate) and -443 mV/SCE (IIIc). In the reversal potential scan there are three complementary anodic peaks at -75 (Ia), -315 (IIa) and -385 mV (IIIa), respectively. The peaks RM and OM correspond to formation and dissolution processes of the massive deposit, respectively.

In order to determine the type of control limiting the UPD process onto gold substrate, the maximum current density (j_p) value associated with peaks I, II and III were plotted as a function of the scan rate (ν). The plot corresponding to the peaks is shown in Fig. 5.

One may note a linear relationship for these processes, suggesting an adsorption-controlled process.

The integration of the cathodic current with respect to time in cyclic voltammetry yields the total charge passed during the scan potential. Subtraction of the double-layer charge from this charge yields the charge associated with that of Tl UPD monolayer. The value determined was $186 \pm 6 \mu C/cm^2$.

Figure 6 shows a set of frequency change vs E curves recorded at different potential limits in the UPD region. In all curves the frequency changes are virtually identical which confirms their reproducibility. Considering the direct scan from 600 mV to -760 mV, the frequency decreases slowly (mass increase) corresponding to UPD process of thallium in different types of adsorption sites onto gold substrate. The total frequency change in this UPD potential region is 21.5 Hz. Following scan reversal at -760 mV, the frequency increases slowly until the original value of frequency is attained at +600 mV.

The value of Δf associated with a thallium monolayer on the substrate can be converted to monolayer charge, ΔQ ($\mu C/cm^2$), using both the Sauerbrey equation (1) and the first Faraday's law:

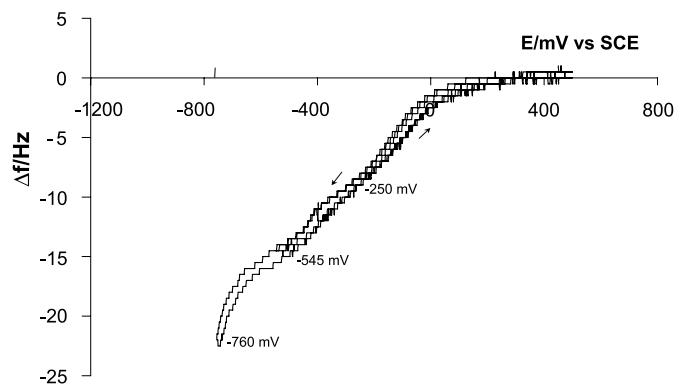


Fig. 6. A set of experimental frequency change vs. E curves recorded at different potential limits in the UPD region indicated in the figure. The scan rate was 5 mV s⁻¹ and these curves were obtained concomitantly with j-E curve in Fig. 4.

$$\Delta m = \frac{MM}{nF} \times \Delta Q \quad (2)$$

$$\Delta f = - \left(\frac{C_f^{-1} MM}{nF} \right) \times \Delta Q \quad (3)$$

In these expressions MM (g mol^{-1}) is the molar mass of the metal, n is the number of electrons involved and the other symbols take their usual significance.

In consequence, 21.5 Hz are equivalent to $178 \mu\text{C}/\text{cm}^2$ which is greater than $155 \mu\text{C}/\text{cm}^2$, reported by Adzic et al. [26] for a close-packed hexagonal monolayer. This discrepancy may be explained by the microroughness in the substrate or by the adsorption of solvent molecules from the electrolyte.

Previous studies [27] of the adsorbed Tl in the UPD region indicate that the deposition begins (peaks I) with the process of thallium adsorption-desorption on the energetically most accessible sites (steps, defects, holes and grain boundaries). Finally the monolayer is completed (peaks II and III) when the thallium atoms occupy the least accessible sites (terraces) on the substrate.

3. Thallium UPD on Au in the Presence of Chloride

3.1. Voltammetric study

Figure 7 shows a set of voltammogram curves (CV) when the UPD process of thallium is produced in the presence of chloride. The chloride concentrations were (a) 0, (b) 10^{-3} and (c) 10^{-2} M in order to eliminate the evolution of Cl_2 and the formation of coordination complexes with the metallic ion.

The first result is that in all voltammetric responses, obtained in the presence of chlorides, there is the same number of peaks as obtained in the absence of chloride anions.

Furthermore, at all anion concentrations the effect of adsorption of chloride anions on the voltammogram is clearly observed to be more important for peak I. When the anion

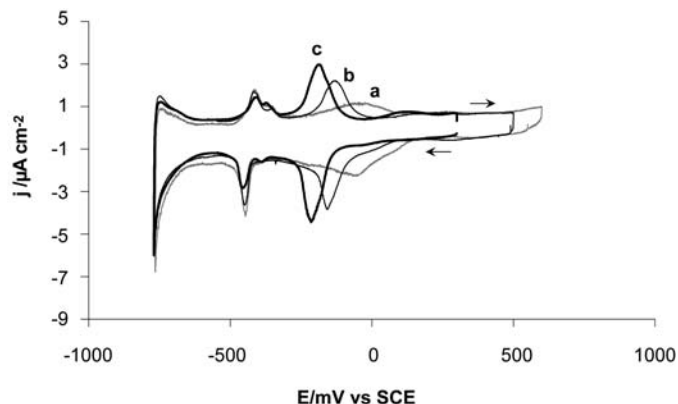


Fig. 7. Cyclic voltammograms, j vs. E , curves recorded in UPD region of Tl/Au system at different chloride concentrations: $\text{Au}/10^{-3} \text{ M Tl}^+ + 1 \text{ M NaClO}_4 + x 10^{-3} \text{ M Cl}^-$ (pH 3.5): a) $x = 0$, b) $x = 1$ y c) $x = 10$. In all curves the scan rate was 5 mV s^{-1} .

concentration increases, the peak I displaces towards more negative values of the potential and its intensity increases. This behavior reflects that Tl-Tl interactions are more intensive than when chloride ions are absent at the electrode surface.

However, the position of peaks III (and II) remains constant at all anion concentrations, but the intensity of peak IIIc diminishes as the chloride concentration increases. In addition to this behavior, the cathodic charge under the peaks I and III diminishes by 3.2% and 22.4%, respectively, for both anion concentrations used as can be seen in Table 1 for the cathodic peaks IIIc and Ic only.

Table 1. Cathodic charge associated with peaks Ic and IIIc at different anion concentrations.

$[\text{Cl}^-] / \text{M}$	$Q(\text{Ic}) / \mu\text{C cm}^{-2}$	$Q(\text{IIIc}) / \mu\text{C cm}^{-2}$
0	-130.8	-58.4
10^{-3}	-125.8	-44.8
10^{-2}	-124.6	-47.6

After considering all the above results, we resumed that:

- The existence of peaks I and III (and II) in the voltammetric responses obtained in the presence of chloride anions reflects that the formation process of thallium UPD on gold is same in the absence or presence of chloride anions at the substrate.
- However, the displacement of peak I towards negative potentials suggests that the chloride anions simply block the adsorption sites for thallium. Moreover, the Tl-Tl interactions are greater in the presence of chloride anions at the substrate with respect to the absence of these anions. The peak I is more affected by this process, since at this potential, chloride anion adsorption is more significant.

3.2. Electrogravimetric study

The application of EQCM technique can provide new complementary information on the effect of chloride anions on thallium UPD process.

The EQCM results are shown in Figure 8. As seen in this figure, the curves obtained in the presence of anions show similar behavior to that defined in two potential regions. For example, if the reference is microgravimetric curve obtained in sodium perchlorate solution in the absence of chloride anions (curve a), the response corresponding to 10^{-3} M chloride concentration displays the first potential region, between 300 mV and -180 mV , where the frequency variation, Δf , remains practically constant. The second region is found at potential values more negative than -180 mV where the curve has the same shape of that corresponding to the absence of chloride anions in solution, but is displaced toward more posi-

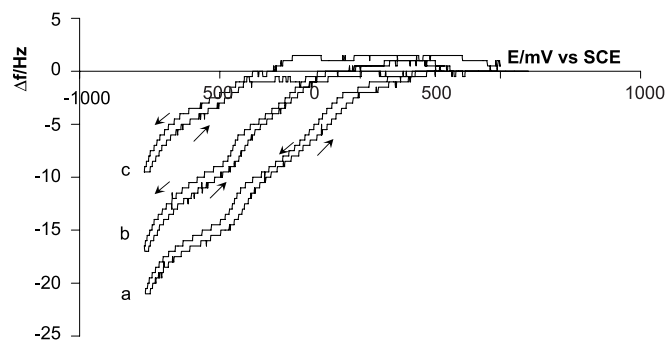


Fig. 8. EQCM Δf data plotted against potential, recorded simultaneously with the cyclic voltammograms in Fig. 7. The potential scan was performed using a 5 mV s^{-1} scan rate.

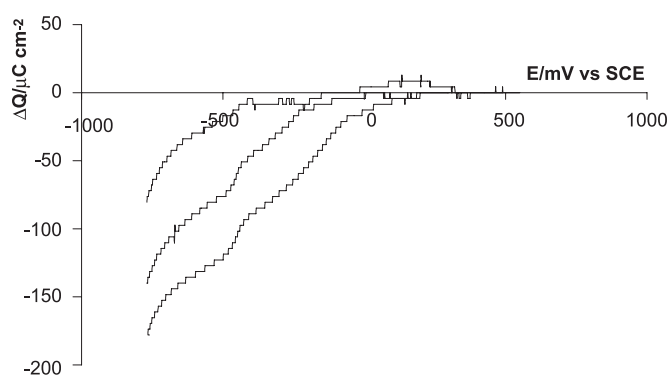


Fig. 9. Curves of the charge on the negative-going sweeps measured using electromicrogravimetric balance as a function of scanned potential for the system Au/10⁻³ M Tl⁺⁺ 1 M NaClO₄ + $x \cdot 10^{-3}$ M Cl⁻ (pH 3.5): a) $x = 0$, b) $x = 1$ and c) $x = 10$. The scan rate used was 5 mV s^{-1} .

tive values of Δf , approximately equal to 4 Hz. For a higher concentration of chloride anions (10^{-2} M), the first potential region ranges between 300 mV and -350 mV and thereafter starts the second towards negative potentials. In this case the curve is shifted for about 11.5 Hz as compared to the response in the absence of anions.

3.2.1. Behavior in the negative-going sweeps

According to the representation of EQCM curves like ΔQ as a function of E in Figure 9, only the negative-going sweeps can generate more information of the effect of anions on the UPD process.

As can be seen in each curve only a “monolayer fraction” is detected by the microbalance. In Table 2 it is possible to observe each “submonolayer” charge at different anion concentrations.

In terms of charge, the microbalance detects only the charge equivalent to 79% and 45% of a thallium monolayer

Table 2. Monolayer charges of thallium as a function of the anion concentration obtained by electromicrogravimetry.

[Cl ⁻]/M	$Q_{\text{Tl(Cl)}}/\mu\text{C cm}^{-2}$
0	-177.9
10^{-3}	-139.8
10^{-2}	-80.5

when the chloride anion is in 10^{-3} M and 10^{-2} M solutions, respectively.

It is necessary to mention that this result does not imply that the thallium monolayer has been formed in part, but that the microbalance detects only a fraction of it, since in Figure 7 the number of peaks and their general shape are almost invariable. This behavior suggests that in the first potential zone both the anion and thallium adsorption occur to form the metallic monolayer. During this process a strong interaction between thallium atoms is produced due the presence of chloride atoms on the adjacent sites. This strong interaction causes that current peaks associated with peak I become much sharper and peak potentials change towards more negative values.

In addition, the potential region in each curve is greater proportionally with anion concentration due to the displacement towards cathodic potentials from the potential of zero charge of the gold substrate. This fact affects the anion desorption at high concentration that is produced at more cathodic potentials with respect to low anion concentrations.

Another way of identifying the chloride effect on thallium UPD is to calculate the molmass $(\text{MM}/n)_{\text{Tl}}$ for the adsorbate species evaluated from the plots of frequency changes against respective integrate change of CV charge, ΔQ_f , in $\mu\text{C cm}^{-2}$ for various Cl⁻ concentrations (Figure 10). This can be evaluated by eq. (3).

Considering that thallium atoms accept 1 electron ($n = 1$) to form the monolayer [26, 28], it is possible to determine

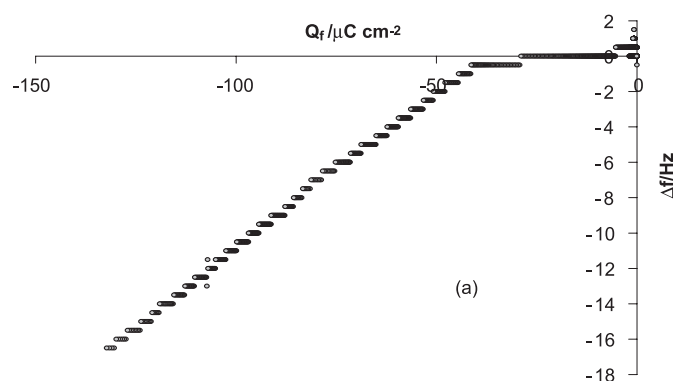


Fig. 10. Plots of frequency changes Δf against respective integrate CV charges ΔQ_f associated with thallium UPD process onto gold in the presence of chloride anions (a) 10^{-3} M and (b) 10^{-2} M.

chloride ions (N_{Cl}) per atom of thallium involved in thallium UPD process:

$$\Delta(MM) = (MM/n)_{Tl} - MM_{Tl} \quad (4)$$

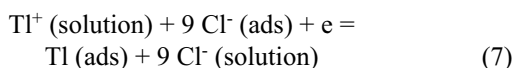
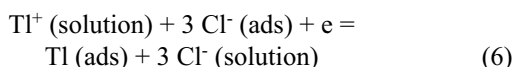
$$N_{Cl} = \Delta(MM)/MM_{Cl} \quad (5)$$

Where $\Delta(MM)$ is the molar mass of chloride adsorbed prior to the onset of UPD process or eliminated upon termination of UPD process; $(MM/n)_{Tl}$ is the molmass of the adsorbate species, MM_{Tl} is the molar mass of thallium (204.4 g mol⁻¹) and MM_{Cl} is the molar mass of chloride ion (35.45 g mol⁻¹).

Note that this determination involved the identification of the slopes of curves ΔQ_f vs Δf , which are shown in Figure 10.

In the light of the curves in Figure 10, there are two slopes corresponding to the peaks on the cyclic voltammograms (see for example figure 7). The results of N_{Cl} obtained at non-zero slopes are tabulated in Table 3.

According to these results, at anion concentration 10⁻³ M, three chloride anions are desorbed when one thallium atom is adsorbed. If the anion concentration is 10⁻² M then nine chloride anions are desorbed per one thallium atom adsorbed. On the basis of our results the following reactions can be attributed to the potential region of peak I used at the respective anion concentrations 10⁻³ and 10⁻² M:



It is interesting to note that this relation is the same for the curve shift observed in the presence of anion as compared to the absence of anions shown in Figure 8.

In considering the latter series of results, the electromicrogravimetric variation of frequency in the presence of coadsorbed anions could be described by the following expression:

$$\Delta f(ClO_4^- + A^-) = \Delta f_{M/Au}(ClO_4^-) + \Delta f_{A^-/Au}(ClO_4^- + A^-) + \Delta f_{A^-/M}(ClO_4^- + A^-) \quad (8)$$

where $\Delta f_{A^-/X}(ClO_4^- + A^-)$ corresponds to the adsorption ($\Delta f > 0$) or desorption ($\Delta f < 0$) of A⁻ anions onto X (X = Au, M) and

$\Delta f_{M/Au}(ClO_4^-)$ is the frequency variation in the absence of specific adsorption. This expression is valid for the case when the adsorption of A⁻ anions onto X is a function of the potential, when the structure of the adsorbed metal layer is same in the presence and absence of A⁻ and when there are no strong interactions between M-Au, and A—Au.

According to equation 8, in the first potential region (pick I) there is

$$\Delta f_{A^-/Au}(ClO_4^- + A^-) + \Delta f_{A^-/M}(ClO_4^- + A^-) \approx \Delta f_{M/Au}(ClO_4^-) \quad (9)$$

for which, the term associated with chloride adsorption on gold electrode, $\Delta f_{A^-/Au}(ClO_4^- + A^-)$, is more important than the term corresponding to its adsorption on thallium, $\Delta f_{A^-/M}(ClO_4^- + A^-)$. For the second potential region (peaks II and III)

$$\Delta f_{A^-/Au}(ClO_4^- + A^-) + \Delta f_{A^-/M}(ClO_4^- + A^-) \approx 0 \quad (10)$$

and the total variation of frequency $\Delta f(ClO_4^- + A^-)$ is given by

$$\Delta f(ClO_4^- + A^-) = \Delta f_{M/Au}(ClO_4^-) \quad (11)$$

For a higher concentration of chloride anions (10⁻² M), the first potential region ranges between 300 mV and -250 mV and the second starts from this latter towards negative potentials and is displaced for about 12 Hz as compared to the response obtained in the absence of anion.

Based on these results, the adsorption of chloride anions on thallium underpotential deposition, according to our model, takes place as follows: first, as the concentration of anions in solution increases, their surface concentration becomes more significant and blocks adsorption sites for the metal ion until the anions are released at increasingly negative values of the potential. Second, as the anion concentration increases, adsorbed anions block the thallium adsorption more intensively. These two phases may be related to the well-known fact that at higher anion concentration, the potential of zero charge displaces toward more negative values delaying the release of the occupied sites [1]. In addition, during the chloride desorption process, thallium adsorption is more intensively masked with increasing anion concentration in solution, which is reflected in practically constant variation of frequency.

Finally, it can be assumed that for the lowest concentration of chloride anions (10⁻³ M) in solution, the amount of anions adsorbed on gold electrode, prior to the beginning of thallium adsorption, may correspond to a layer of chloride anions with (1x1) structure or to a fraction of a compact layer of chloride anions with a Cl-Cl separation of 2.02 Å [29], since the variation of frequency in the first case is equal to 4.6 Hz, and in the second, to 8.1 Hz.

Regarding the second concentration of chloride anions used (10⁻² M), and not taking into account the amount adsorbed on thallium atoms mentioned above, these species are more strongly adsorbed and the amount adsorbed can reach more than one compact layer.

Table 3. Molar mass values (ΔMM) of chloride adsorbed prior to the onset of UPD process or eliminated upon termination of UPD process, molmass of the adsorbate species $(MM/n)_{Tl}$ and chloride ions (N_{Cl}) per atom of thallium involved in thallium UPD process

$[Cl^-] / M$	$(MM/n)_{Tl} / g \text{ mol}^{-1}$	$\Delta MM / g \text{ mol}^{-1}$	N_{Cl}
10 ⁻³	305.5	101.2	~3
10 ⁻²	522.7	318.3	~9

Conclusions

The application of EQCM technique coupled with voltammetry provides results for Cl⁻ ion competitive adsorption effect on UPD process of thallium onto gold.

Voltammetric results obtained show a greater effect of chloride anions on underpotential deposit formation of thallium onto gold. The most affected sites on the electrode are thereby grain boundaries, holes and steps; whereas terrace-like sites are minimally affected. Furthermore, during anion desorption process metal atoms occupy the vacated sites, thus evidencing a simultaneous occurrence of these two processes.

Electromicrogravimetric results obtained show that at anion concentration 10⁻³ M, three chloride anions are desorbed when one thallium atom is adsorbed. If the anions concentration is 10⁻² M, then nine chloride anions are desorbed per one thallium atom adsorbed.

Acknowledgements

A. M-R is grateful to CONACYT for the scholarship given in support of this work.

References

1. Kolb, D. M., in: *Advances in Electrochemistry and Electrochemical Engineering*, Vol. 11, John Wiley and Sons, USA, **1978**.
2. Aramata, A., in: *Modern Aspects of Electrochemistry*, No. 31, Plenum Press, USA, **1997**.
3. Adzic, R., in *Electrocatalysis*, Lipkowski, J.; Ross, P. N. Eds., Wiley-VCH, New York, **1998**, Chap. 5
4. Wheeler, D. R.; Wang, J. X.; Adzic, R. R. *J. Electroanal. Chem.*, **1995**, 387, 115.
5. Stadler, R.; Jusys, Z.; Baltruschat, H. *Electrochim. Acta*, **2002**, 47, 4485.
6. Horanyi, G. Vertes, G. *J. Electroanal. Chem.*, **1973**, 74, 705.
7. Samant, M. G.; Toney, M. F.; Borges, G. L.; Blum, L.; Melroy, O. R. *J. Phys. Chem.* **1988**, 92, 220-225.
8. Jovic, V. D.; Jovic, B. M. *Electrochim. Acta*, **2002**, 47, 1777-1785.
9. Takahashi, S.; Hasabe, K.; Aramata, K. *Electrochem. Comm.* **1999**, 1, 301-304.
10. Hepel, M.; Kanige, K.; Bruckenstein, S. *Langmuir* **1990**, 6, 1063-1067.
11. Jusys, Z.; Bruckenstein, S. *Electrochem. Comm.* **2000**, 2, 412-416.
12. Markovic N., Ross P. N. *Langmuir*, **1993**, 9, 580.
13. Schmidt, E., Wuthrich, N. *J. Electroanal. Chem.*, **1970**, 28, 349.
14. Kolb, D.; Przasnyski, M.; Gerischer, H. *Elektrokhimiya* **1977**, 13, 700.
15. Schultze, J.; Vetter, K. *Electrochim. Acta* **1975**, 19, 915.
16. Juttner, K.; Lorenz, W.; Staikov, G.; Budevski, E. *Electrochim. Acta*, **1978**, 23, 741.
17. Kolb, D.; Al Jaaf-Golze, K.; Zei, M. *Dechema-Monographien*; Verlag Chemie: Weinheim, **1986**, Vol 12, p. 53.
18. Buttry, D. A., in: *Electroanalytical Chemistry*, Vol. 17, Bard, A. J., Ed., Marcel Dekker Inc., New York, **1991**.
19. Hepel, M., in: *Interfacial Electrochemistry, Theory, Experiment and Applications*, Wieckowski, A. Ed., Marcel Dekker, Inc. New York, **1999**.
20. Niece, B. K.; Gewirth, A. A. *J. Phys. Chem. B.* **1998**, 102, 818.
21. Clavilier, J.; Nguyen van Huong, C. *J. Electroanal. Chem.* **1977**, 80, 101-114.
22. Hamelin, A.; Katayama, A.; Picq, G.; Vennereau, P. *J. Electroanal. Chem.* **1980**, 113, 293-300.
23. Hamelin, A. *J. Electroanal. Chem.* **1979**, 101, 285-290.
24. Montes-Rojas, A. Thèse de doctorat, Université Joseph Fourier-Grenoble 1, Grenoble France, **2000**.
25. Snook, G. A.; Bond, A. M.; Fletcher, S. *J. Electroanal. Chem.* **2002**, 526, 1.
26. Adzic, R. R.; Wang, J.; Ocko, B. M., *Electrochim. Acta* **1995**, 40, 83.
27. Wang, J. X.; Adzic, R. R.; Ocko, B. M. *J. Phys. Chem.* **1994**, 98, 7182
28. Engelsmann, K.; Lorenz, W. J.; Schmidt, E. *J. Electroanal. Chem.* **1980**, 114, 1.
29. Kittel, C., in: *Physique de l'Etat Solide*, Dunod, Francia, **1998**, p. 59.